

Multicolour modelling of SN 2013dx associated with GRB 130702A

A. Volnova,^{1*} M. Pruzhinskaya,^{2,3*} A. Pozanenko,^{1,4,5} S. Blinnikov,^{6,7,8} P. Minaev,¹ O. Burkhonov,⁹ A. Chernenko,¹ Sh. Ehgamberdiev,⁹ R. Inasaridze,¹⁰ M. Jelinek,¹¹ G. Khorunzhev,¹ E. Klunko,¹² Yu. Krugly,¹³ E. Mazaeva,¹ V. Rumyantsev,¹⁴ A. Volvach¹⁴

¹ - Space Research Institute, Moscow, Russia; ² - Lomonosov Moscow State University, Sternberg Astronomical Institute, Moscow, Russia; ³ - Laboratoire de Physique Corpusculaire, Université Clermont Auvergne, Clermont-Ferrand, France; ⁴ - National Research Nuclear University MEPhI (Moscow Engineering Physics Institute), Moscow, Russia; ⁵ - Moscow Institute of Physics and Technology, Dolgoprudny, Moscow Region, Russia; ⁶ - Institute for Theoretical and Experimental Physics, Moscow, Russia; ⁷ - All-Russia Research Institute of Automatics, Moscow, Russia; ⁸ - Kavli Institute for the Physics and Mathematics of the Universe (WPI), The University of Tokyo Institutes for Advanced Study, The University of Tokyo, Kashiwa, Japan; ⁹ - Ulugh Beg Astronomical Institute (UBAI) of the Uzbek Academy of Sciences, Tashkent, Uzbekistan; ¹⁰ - Khardze Abastumani Astrophysical Observatory, Iliia State University, Tbilisi, Georgia; ¹¹ - Astronomical Institute of the Czech Academy of Sciences, Ondřejov, Czech Republic; ¹² - Institute of Solar-Terrestrial Physics, Russian Academy of Sciences, Siberian branch, Irkutsk, Russia; ¹³ - Kharkiv National University, Institute of Astronomy, Kharkiv, Ukraine; ¹⁴ - Crimean Astrophysical Observatory of the Russian Academy of Sciences, Crimea, Nauchny, Russia; * e-mail: alinuuss@gmail.com, pruzhinskaya@gmail.com

The light curve of SN 2013dx associated with GRB 130702A is the second well sampled GRB-SN after SN 1998bw. We collected all available optical data of this event: the multicolour light curves of GRB 130702A contain 330 data points in filters *uBgrRiz* until 88 days after the burst start, more than 280 of them form the light curves of the associated supernova SN 2013dx (Fig.1) [5,9,10].

We present the multicolour light curves of this SN, modelled with the code STELLA [2,3]. STELLA is a package of one-dimensional spherically symmetrical multi-group radiation hydrodynamics code which treats non-equilibrium radiative transfer according to chemical composition and inner structure of a pre-SN star. The code has been used for light curve modelling of different types of SNe (Ia – [3]; Ib/Ic – [6,7]; IIc – [4]; IIb – [2]; IIP- [1,8]). The assumptions about the supernova outburst geometry are also simple like in the empirical method, but the consideration of chemical abundances and distribution of different chemical elements inside a pre-SN star allows one to calculate radiative transfer during the explosion and to build more physically correct modelled light curve. The model in filters as well as the quasibolometric light curve (Fig.2) is in a fairly good agreement with the observations. The STELLA predictions of photospheric velocities fit well the ones obtained from spectra (Fig.3). The bolometric parameters of the supernova according to the model are: the pre-SN mass and radius $M = 25 M_{\odot}$, $R = 100 R_{\odot}$; the mass of the compact remnant $M_{CR} = 6 M_{\odot}$, the energy of the SN explosion $E_{\text{oburst}} = 3.5 \times 10^{52}$ erg, the mass of synthesized $M_{56\text{Ni}} = 0.2 M_{\odot}$ and it is totally mixed inside the envelope; the chemical abundances in the pre-SN are $M_{\text{O}} = 16.6 M_{\odot}$, $M_{\text{Si}} = 1.2 M_{\odot}$, and $M_{\text{Fe}} = 1.2 M_{\odot}$. The pre-supernova star mass and radius varies in the range 23–27 M_{\odot} and 75–125 R_{\odot} , respectively; the ^{56}Ni mass lies between 0.15 and 0.25 M_{\odot} ; and the explosion energy E_{oburst} in the range of (30–40) $\times 10^{51}$ erg. The influence of different input parameters is shown in the Fig.4.

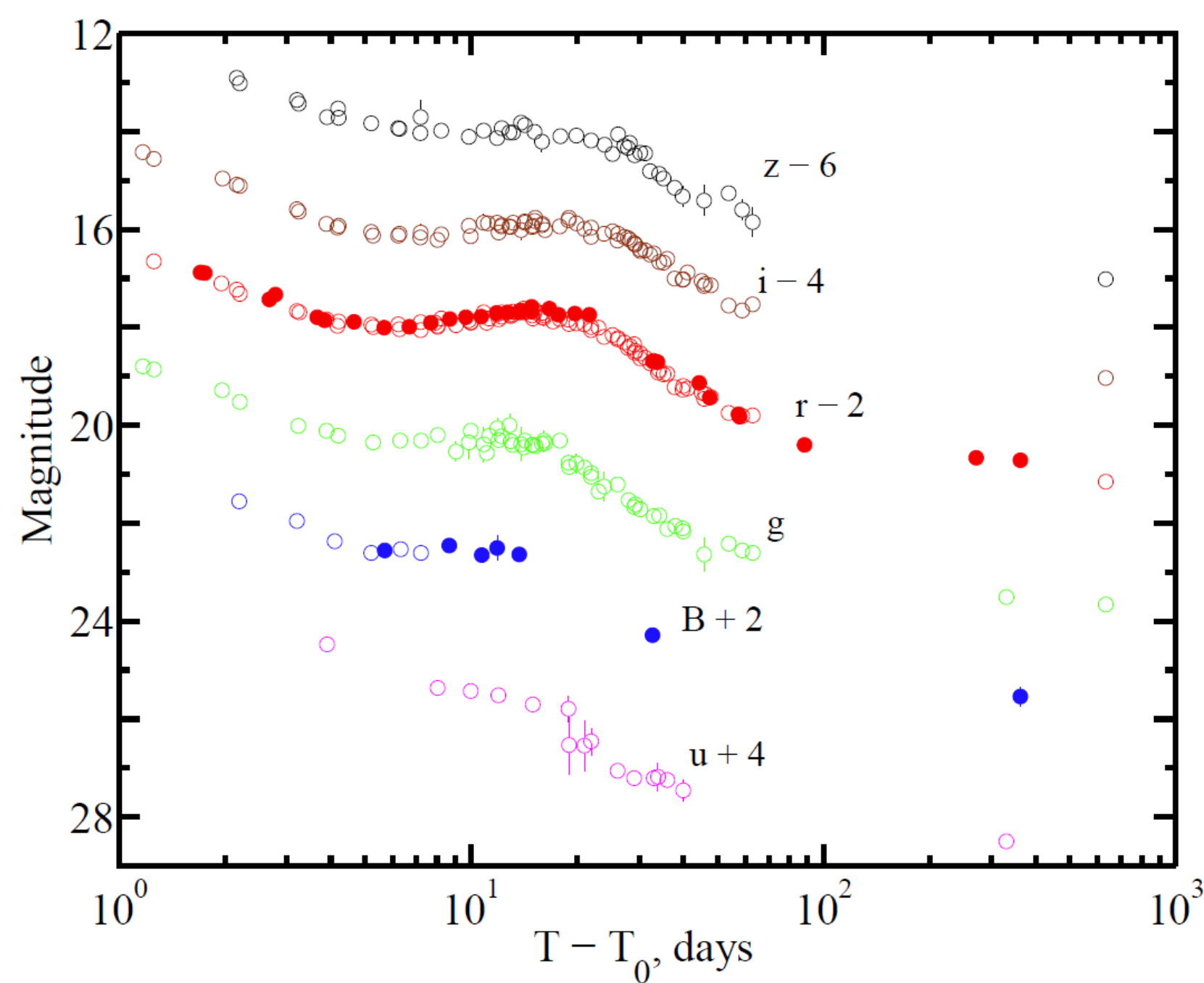


Fig. 1. The observed multicolour light curves of SN 2013dx associated with GRB 130702A contain 330 data points in filters *uBgrRiz* until 88 days after the burst start, more than 280 of them form the light curves of the associated supernova SN 2013dx. 40 of these points are published for the first time. Filled circles present the observational data of our GRB-follow-up collaboration, and open circles depict the data collected from the literature [5,9,10]. The supernova phenomenon is clearly seen in every filter. Galactic extinction is not taken into account.

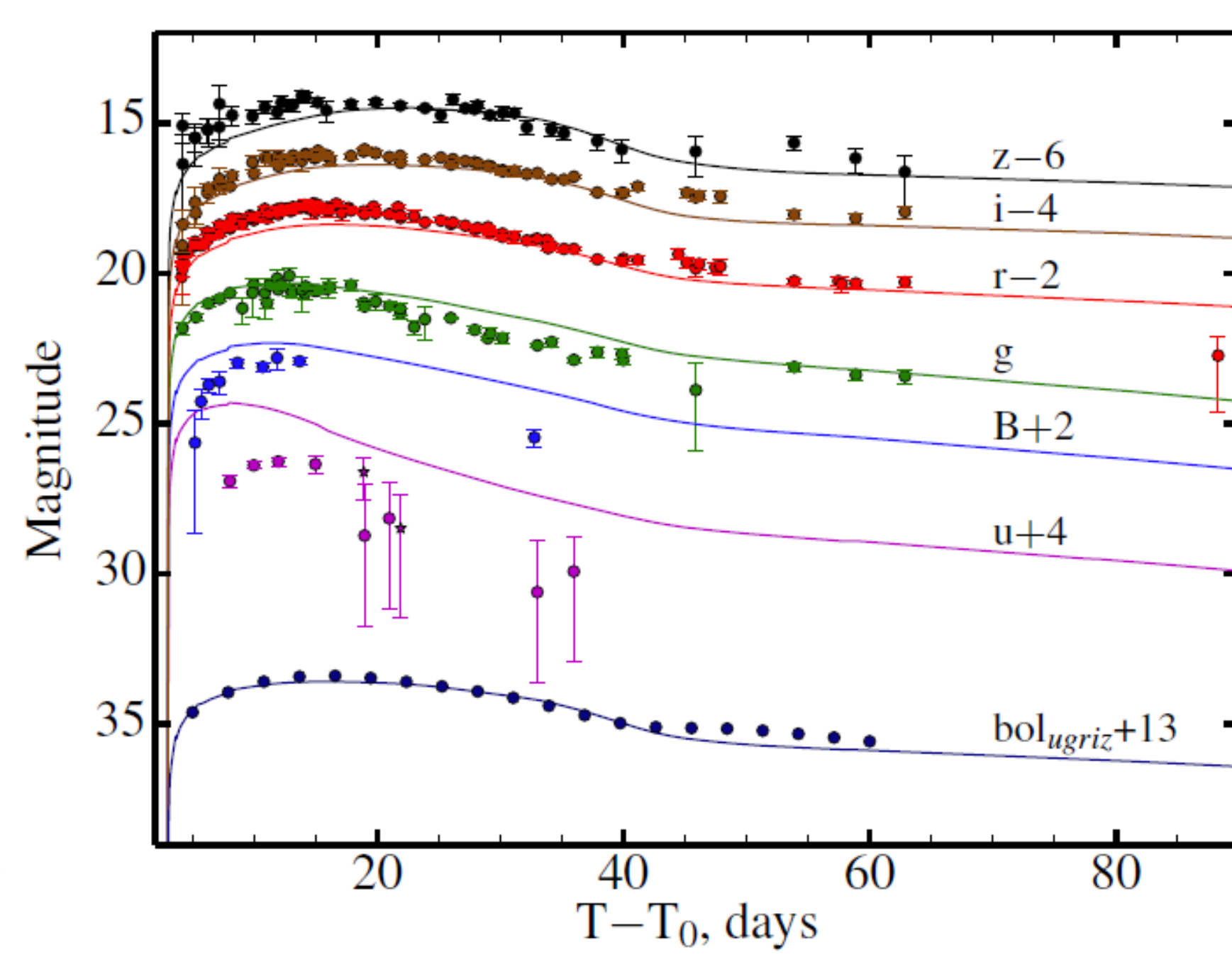


Fig. 2. The multicolour light curves of SN 2013dx. The Galactic extinction, the flux from the host galaxy and the optical afterglow contribution are excluded. Solid lines show the best model of the SN light curve obtained by STELLA [2,3]. The quasibolometric light curve of the SN in AB photometric system obtained as a sum of the fluxes in *ugriz* filters, is marked as *bol_ugriz*. The data and model are in observer frame. The best model parameters of the pre-SN star and its remnant are collected in Table 1.

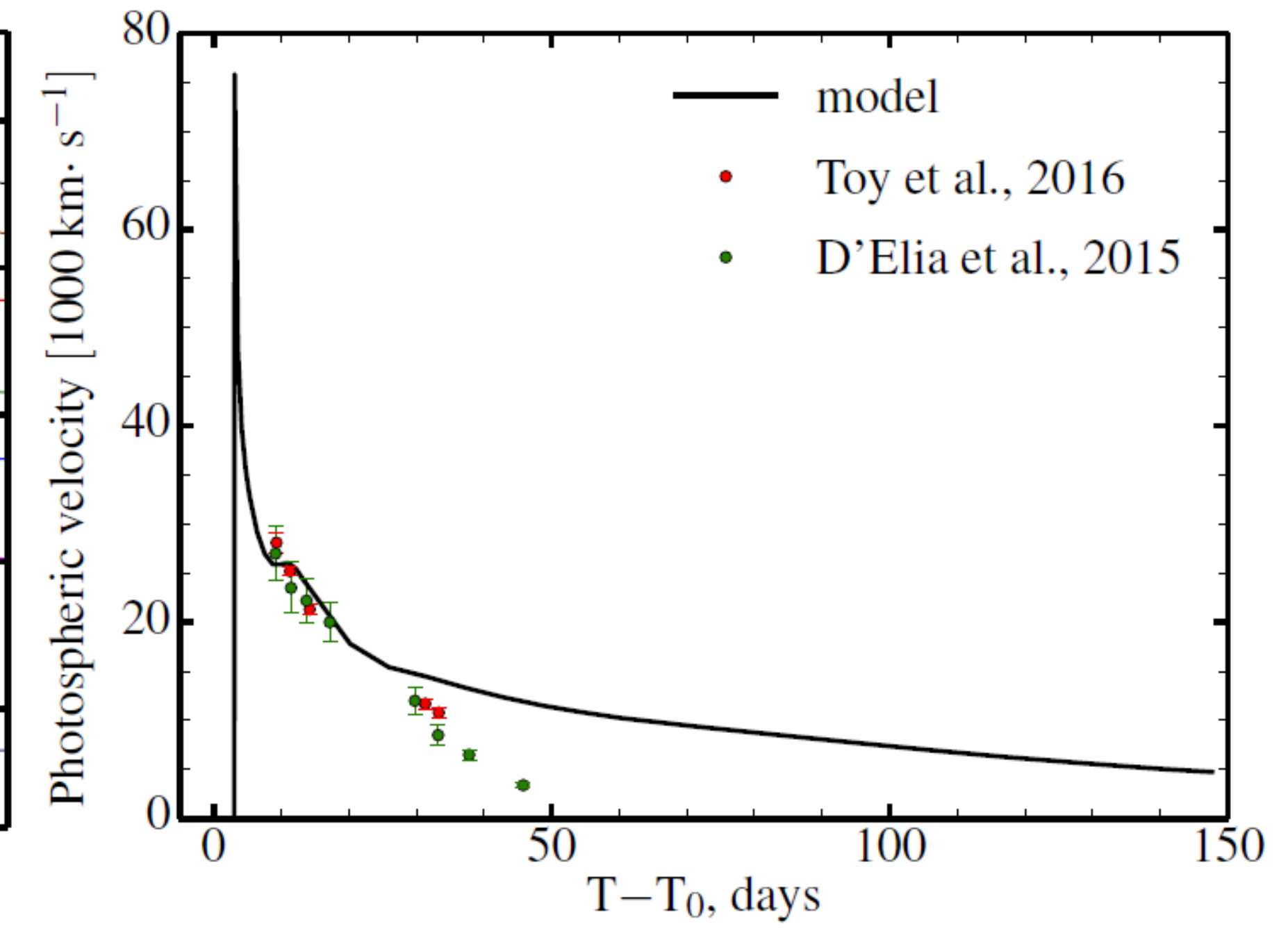


Fig. 3. The evolution of photospheric velocities of SN 2013dx measured via observations (points) [5,9] and calculated from the modelling (solid line). The plot is in observer frame. The model evolution of the photospheric velocities is in good agreement with direct observations during the first ~30 days after the explosion.

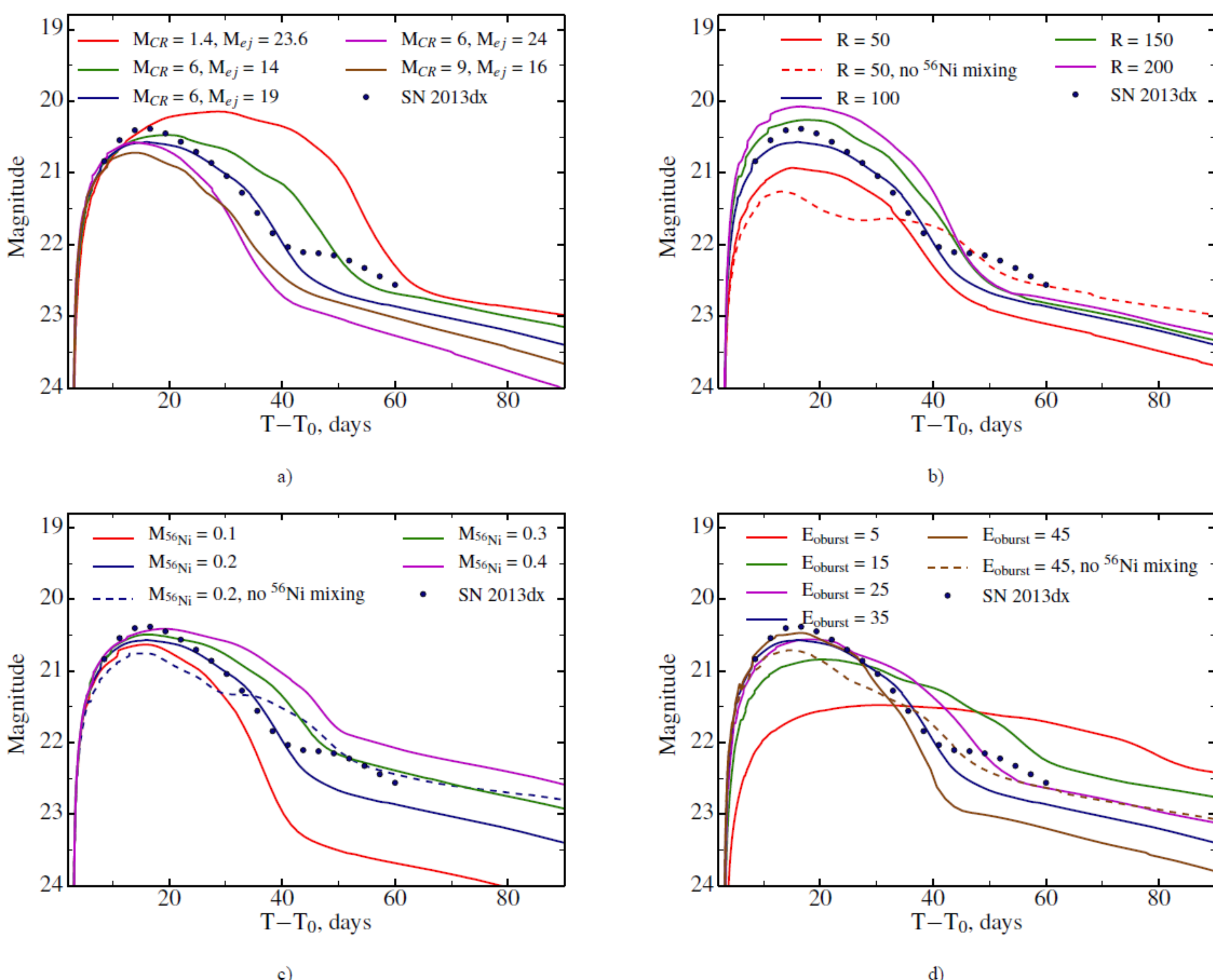


Fig. 4. The dependence of the quasibolometric light curve (*ugriz* filters) on the different parameters of the optimal model (dark blue curve): a) the mass of the pre-supernova star and its distribution between the ejecta and the compact remnant (here and in other panels masses are in units of M_{\odot}); b) the radius of the pre-supernova star in units of R_{\odot} ; c) the mass of the synthesized ^{56}Ni ; d) the energy of the outburst in units of 10^{51} erg. Filled circles show the observational quasibolometric light curve of the SN 2013dx. ^{56}Ni is totally mixed through the ejecta for all presented models except the models shown with dashed line. The ejecta mass affects the descending part of light curve, dependence of radius is stronger on the domes of light curve, however, the tail is mainly determined by ^{56}Ni abundance. The models are brighter for higher ejecta or ^{56}Ni mass, and larger radius. The decrease of the compact remnant mass provides wider maximum of the light curve. In panels b,c,d we also present the models with the same amount of ^{56}Ni as our optimal model (0.2 M_{\odot}) but with and without mixing through the ejecta. When ^{56}Ni is mixed, the light-curve maximum is brighter. Moreover, the gamma photons from radioactive decay are not trapped inside an envelope and do not heat the ejecta. Therefore, a photosphere goes faster to the centre and the SNe becomes dimmer on the tail. Decreasing the outburst energy makes the diffusion time of gamma-photons from radioactive decay longer. This manifests itself as a widening of the light curve, moreover, the diminution of decline rate occurs later.

Table 1. A summary of the SN 2013dx parameters obtained by STELLA in comparison with those of other studies (D15 [5]; T16 [9]). All masses are in M_{\odot} . The mass M_{CR} in the central part of a pre-supernova star with a fixed radius (which is much less than the outer radius of the star) is treated as a point-like source of gravity which has a non-negligible influence on expansion of the innermost layers of SN ejecta. The explosion is initiated by putting thermal energy to the innermost layers. The ejecta of SNe has the same chemical composition as pre-supernova star except for ^{56}Ni , because we do not follow the explosive nucleosynthesis. ^{56}Ni can be put in the centre of SN ejecta in the calculations as well as be spread out within any region. We also performed the LC modelling adopting supernova explosion parameters from [9] (^{56}Ni is located in the centre of explosion and no mixing, there is no compact object at all, the initial radius before explosion is small, we put $R = 10 R_{\odot}$). In the early phases the modelled light curves lie below the observational ones in all filters. Starting from ~30 day after the explosion *z*, *i*, *r*, and quasibolometric modelled light curves fit sufficiently well the observational data.

Parameter	STELLA model	D15	T16
M	25	$\sim 25 - 30^a$	–
M_{CR}	6	–	–
E_{oburst}	3.5×10^{52} erg	$\sim 3.5 \times 10^{52}$ erg	$(8.2 \pm 0.4) \times 10^{51}$ erg
M_{ej}	19	~ 7	3.1 ± 0.1
R	$100 R_{\odot}$	–	–
$M_{56\text{Ni}}$	0.2, totally mixed	~ 0.2	0.37 ± 0.01
M_{O}	16.6	–	–
M_{Si}	1.2	–	–
M_{Fe}	1.2	–	–
E_{bol}	3.1×10^{49} erg	–	–
t_{peak}	14.35* d	$15 \pm 1^{**}$ d	$13.2 \pm 0.3^{**}$ d

^a - mass of the progenitor on the main sequence

* - on the bolometric light curve

** - on the light curve in the filter *r*

Remaining questions

- There is a problem with simultaneous fitting of observational data in all filters. The time position of the maximum in the modelled and observational LCs does not coincide in every colour, especially in blue ones.
- Despite the modelled quasibolometric LC fits well observational data, the multicolour model does not fit well the peak of the SN in blue filters. The discrepancy between observational points in *B* and *u* filters and resulting modelled LCs may be explained by additional absorption along the line of sight which is not included in the host extinction.
- The resulting model does not describe the secondary bump observed during the SN decay phase clearly visible in red filters between 40 and 60 days after the trigger (see Fig. 4a). The bump may not be related to the SN, but to the afterglow. In this case it may be explained as an interaction of the ejecta with some inhomogeneities in the surrounding interstellar medium, e. g., dense interstellar clouds. For more detailed discussion see [11].

References

- Baklanov P.V., Blinnikov S.I., and Pavlyuk N.N., 2005, *AstL*, 31,429
- Blinnikov S. I., Eastman R., Bartunov O. S., Popolitov V. A., Woosley S.E., 1998, *ApJ*, 496, 454
- Blinnikov S. I., Röpke F. K., Sorokina E. I., et al., 2006, *A&A*, 453, 229
- Chugai N.N., Blinnikov S.I., Cumming R.J., et al., 2004, *MNRAS*, 352, 1213
- D'Elia V., Pian E., Melandri A., et al., 2015, *A&A*, 577, A116
- Folatelli G., Contreras C., Phillips M., et al., 2006, *ApJ*, 641, 1039
- Tauris T. M., Langer N., Moriya T. J., et al., 2013, *ApJ*, 778, 23
- Tominaga N., Blinnikov S., Baklanov P., et al., 2009, *ApJ*, 705, 10
- Toy V. L., Cenko S. B., Silverman J. M., et al., 2016, *ApJ*, 818, id.79
- Singer L. P., Cenko S. B., Kasliwal M. M., et al., 2013b, *ApJL*, 776, L34
- Volnova A. A., Pruzhinskaya M. V., Pozanenko A. S., et al., 2017, *MNRAS*, 467, 3500